Jour. Indian Association of Sedimentologists, Vol. 35, No. 2 (2018) Special Issue dedicated to George Devries Klein in celebrating his life and achievements pp 13 - 32 *ISSN 0970-3268*

Bioturbation and trace fossils in deep-water contourites, turbidites, and hyperpycnites: A cautionary note

G. Shanmugam
Department of Earth and Environmental Sciences, The University of Texas at Arlington, Arlington, TX 76019, USA
E-mail: shanshanmugam@aol.com

Abstract: Bioturbation and trace fossils have been claimed to be an important attribute of deep-water contourites, turbidites, and hyperpycnites. However, these biogenic features have nothing to do with fluid mechanics of depositional processes of contour currents, turbidity currents, or hyperpycnal flows. Bioturbation can be both syn- and post-depositional in timing. Therefore, the presence of ichnological signatures in the ancient sedimentary record is irrelevant for interpreting deep-water deposits as a product of a specific process.

Keywords: Bioturbation; Contourites; Hyperpycnites; Trace fossils; Turbidites

Introduction

Since the birth of modern deep-sea exploration by the voyage of H.M.S. Challenger (December 21, 1872–May 24, 1876), organized by the Royal Society of London and the Royal Navy (Murray and Renard, 1891), oceanographers and sedimentologists have made considerable progress in understanding the world's oceans and related deposits. Nevertheless, the physical processes that are responsible for transporting sediment downslope into the deep sea are still poorly understood. This is simply because the physics and hydrodynamics of these processes are difficult to observe and measure directly in deep-marine environments.

During the past five decades, there have been claims on the relationship between ichnological facies and sedimentary environments (Seilacher, 1964; Ager, 1971; Nilsen and Abbott, 1979; Gonthier et al., 1984; MacEachern et al., 2010; Greene et al., 2012; Knaust, 2012; among others). Ichnological signatures (bioturbation and trace fossils) are common in a variety of depositional facies, such as turbidites (Nilsen and Abbott, 1979), contourites (Gonthier et al., 1984; Wetzel et al., 2008; Rodríguez-Tovar and Hernández-Molina, 2018a), tempestites (Ager, 1971; Zhao et al., 2017), hyperpycnites (Mulder et al., 2003; Buatois et al., 2011), and even seismites (Moretti, 2000; Fortuin and Dabrio, 2008; see also Shanmugam, 2016a). The fundamental issues here are:

1) Are bioturbation and trace fossils controlled by fluid mechanics of a specific process?
2) If fluid mechanics do control ichnological signatures, how to distinguish the contourite facies from the associated facies, such as turbidites and hyperpycnites on the basis of bioturnation and trace fossils?

The above two basic issues are still unresolved (Shanmugam, 2016b). Amid this knowledge vacuum, Rodríguez-Tovar and Hernández-Molina (2018a) have published a paper entitled "Ichnological analysis of contourites: Past, present and future". Clearly, the impressive title implies the global importance of ichnological analysis of contourites. However, their theoretical approach, without empirical data, is misleading. Therefore, the primary purpose of this paper is to point out some basic problems in emphasizing the importance of ichnofacies in contourites, and associated turbidites and hyperpycnites. In this regard, I will review the basics of what we know and what we don't know in each case. Hopefully, this cautionary note would deter future workers from promoting the flawed link between

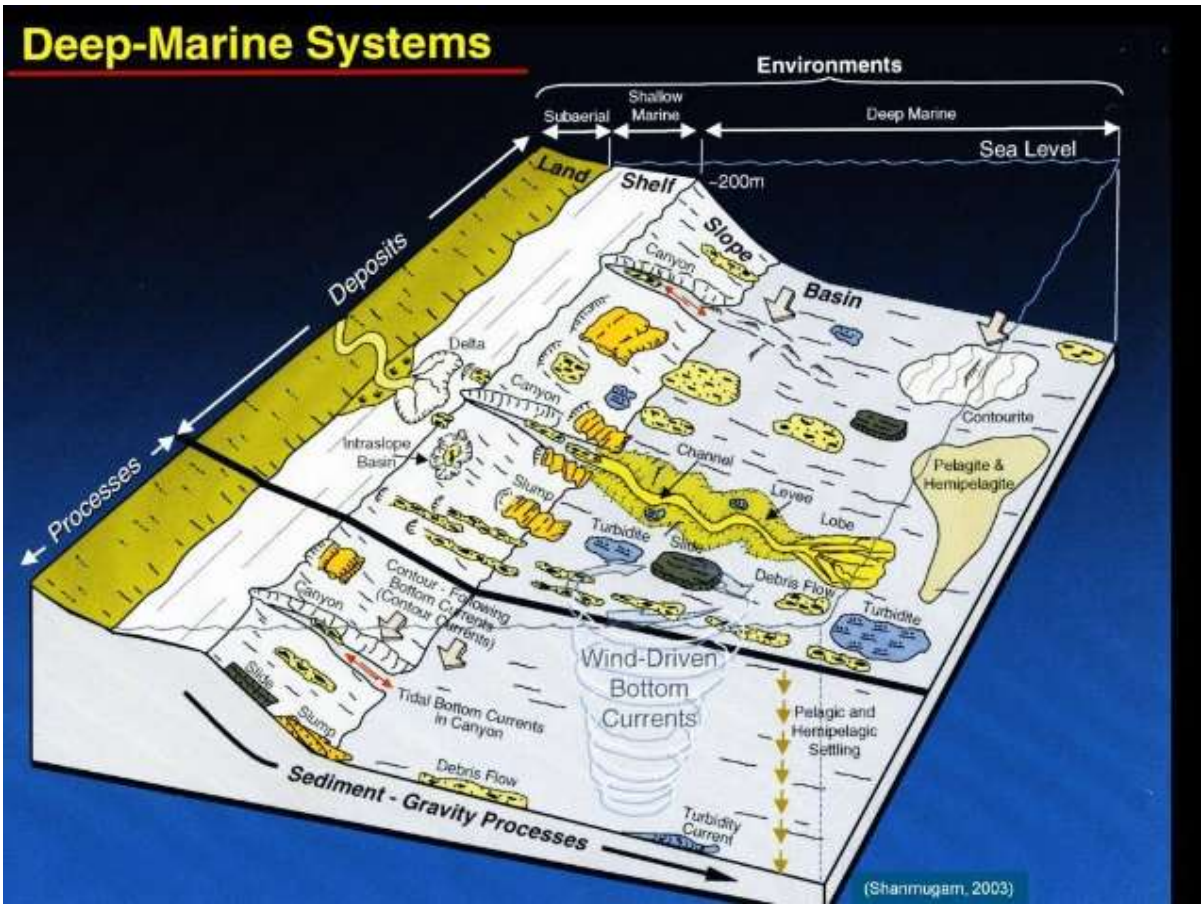

Fig. 1. Schematic diagram showing complex deep-marine sedimentary environments occurring at water depths deeper than 200m (shelf-slope break). In general, sediment transport in shallow-marine (shelf) environments is characterized by tides and waves, whereas sediment transport in deep-marine (slope and basin) environments is characterized by gravity-driven downslope processes, such as mass transport (i.e., slides, slumps, and debris flows), and turbidity currents. Bottom currents, composed of thermohaline contour-following currents, wind-driven currents (circular motion), up and down tidal bottom currents in submarine canyons (opposing arrows), and baroclinic currents (not shown) related to internal waves/tides (Shanmugam, 2013). From Shanmugam (2003). Elsevier.

ichnology and a specific deep-water depositional facies.

Deep-water processes

Deep-water environments (> 200 m in bathymetry, seaward of the continental shelf) are characterized by gravity-driven downslope processes, which comprise slides, slumps, debris flows, and turbidity currents (Fig. 1). In addition, there are four basic types of deep-water bottom currents, namely (1) thermohaline-induced geostrophic bottom currents (contour currents), (2) wind-driven bottom currents, (3) tidal bottom currents, and (4) baroclinic currents associated with internal waves and

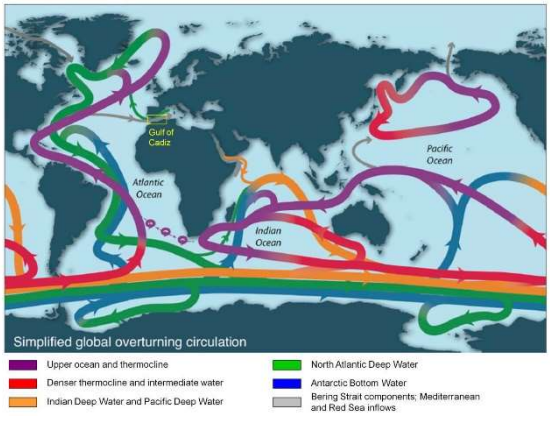

Fig. 2. Map showing the global overturning circulation (GOC). The location of Gulf of Cadiz is added in this article. This site served as the type locality for the contourite facies model odified after Talley (2013), with permission from the Oceanography Society.

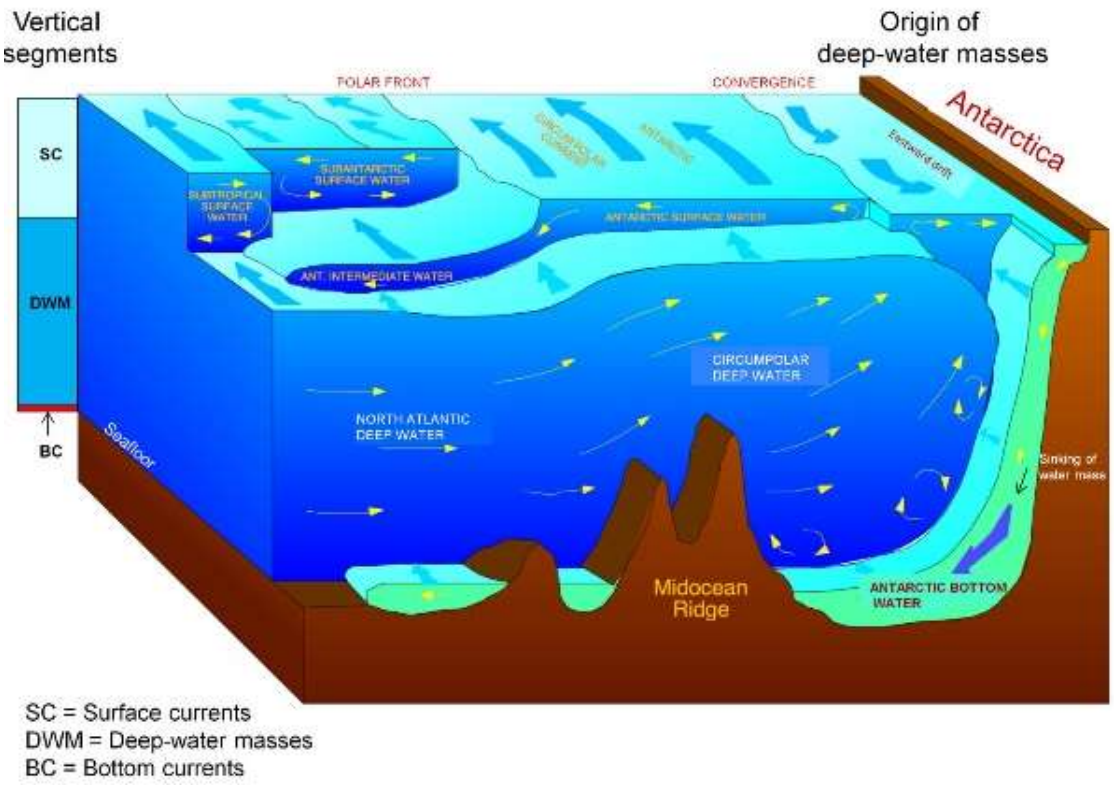

Fig. 3. A conceptual model of the Southern Ocean showing three vertical segments, composed of the upper surface currents, the middle deep-water masses, and the lower bottom currents, forming a vertical continuum (left). Note the origin of AABW by freezing of shelf waters (right). As a consequence, the increase in the density of cold saline (i.e., thermohaline) water triggers the sinking of the water mass down the continental slope and the spreading of the water masses to other parts of the ocean. Modified after Hannes Grobe, September 5, 2015. From Shanmugam (2012), with permission from Elsevier.

tides (Shanmugam, 2012, 2013). Also, Mulder et al. (2003) consider river-deriver hyperpycnal flows reach the deep sea. In this article, deposits of contour currents (i.e., contourites), turbidity currents (i.e., turbidites), and hyperpycnal flows (i.e., hyperpycnites) are the focus.

Contourites The thermohaline circulation (Fig. 2) and related deep-marine bottom currents (Fig. 3) in modern oceans became popular when Heezen et al. (1966) reported deep-water masses and related contour currents along the continental rise in the U.S. Atlantic margin. An example of such deep-water mass is the Antarctic Bottom Water (Fig. 3). In the U. S. Atlantic margin, both downslope- and alongslope- processes have been documented (Fig. 4). Hollister (1967), based on his detailed core study of the U. S. Atlantic margin, introduced the genetic term 'contourite' for deposits of

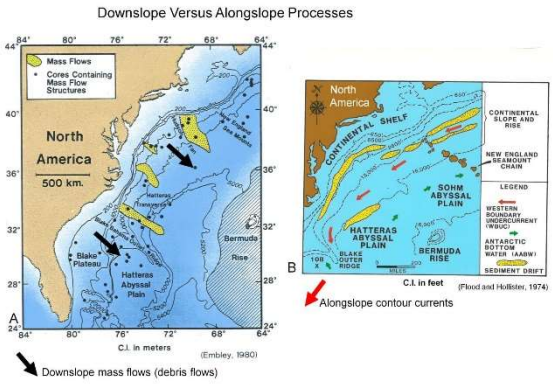

Fig. 4. Comparison of processes on the U.S. Atlantic Margin. A. Downslope mass flows and their deposits (i.e., debrites) (Embley, 1980). B. Alongslope contour currents and their deposits (i.e., contourites) (Flood and Hollister, 1974).

thermohaline-induced geostrophic contour currents in the deep oceans.

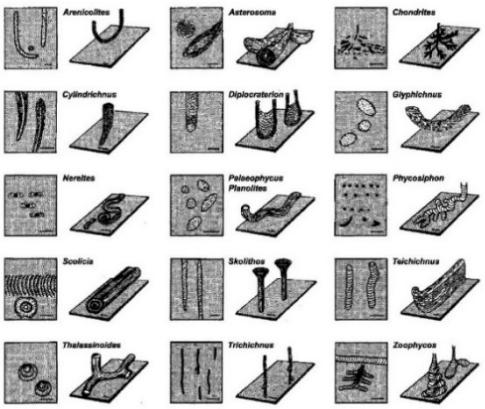

Fig. 5. Trace fossils commonly encountered in contourites. From Wezel et al. (2008).

Wetzel et al. (2008) have documented ichnological signatures in contourites (Figs.

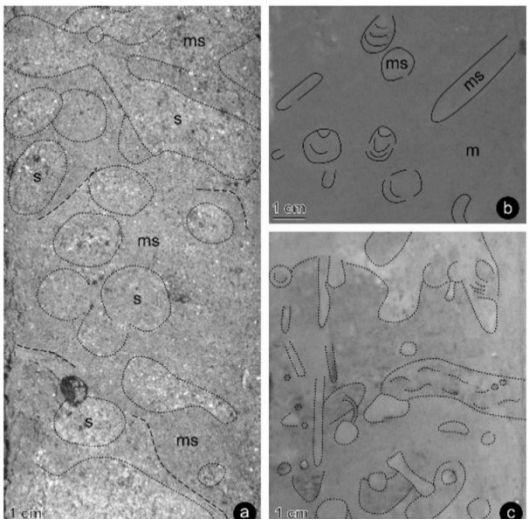

Fig. 6. Glacigenic sediments interpreted as contourites from the Iceland Shetland Channel. **(a)** Sand-rich facies, current-reworked sediments have been mixed by bioturbation to muddy sand (ms); subsequently, sand-enriched burrows (s) were produced. British Geological Survey core 61-04/39 (61°03.5' N, 3°25.1' W; 1125 m water depth) 274-290 cm (Late Pleistocene). **(b)** Sandy mud facies; sands have been mixed into mud, after a early phase of homogenization producing uniform sandy mud (m), distinct burrows containing some more sand (ms) have been formed, which may be ascribed to *Teichichnus* or *Thalassinoides*. **(c)** Muddy facies, light mud resting on grey mud, the contact has been heavily bioturbated, vertical tubes and halo burrows (*Palaeophycus*, *Planolites*, *Thalassinoides*) are common; British Geological Survey core 60. From

5 and 6). Although Rodríguez-Tovar and Hernández-Molina (2018a) have provided an in-depth discussion of terminologies associated with ichnological analysis, they have ignored the very basic conceptual and terminological issues associated with the term 'contourites'.

Consequently, important unresolved issues still exist:

- Contour currents and turbidity currents flow at right angle to each other (Fig. 7). Deposits of these

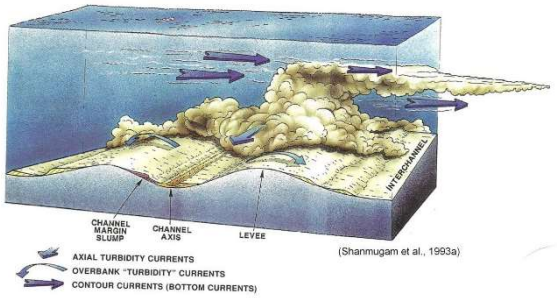

Fig. 7. Conceptual model showing the spatial relationship between downslope turbidity currents and along-slope contour currents. After Shanmugam et al. (1993), AAPG.

hybrid flows at their intersection are poorly understood.

- Gulf of Cadiz (Fig. 8), which served as the type locality for the

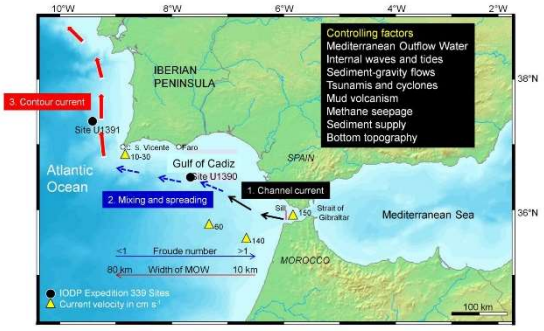

Fig. 8. Schematic diagram showing the location of Gulf of Cadiz and complex transport nature of the Mediterranean Outflow Water (MOW), involving three stages of evolution: (1) channel-current stage, (2) mixing and spreading (i.e., transition) stage, and (3) genuine contour-current stage (see Zenk, 2008, his Fig. 4.10). Figure from Shanmugam (2016b), with permission from Elsevier.

contourite facie model (Fig. 9) (Faugères et al. 1984; Gonthier et al. 1984), is a highly complicated oceanographic location for studying depositional and erosional aspects of genuine contour currents.

Although the Mediterranean Outflow Water (MOW) is considered to be the primary process of deposition of contourites, MOW is not a genuine contour current in the Gulf of Cadiz (Zenk 2008). It evolves through three stages, namely (1) channel current, (2) mixing and spreading, and (3) contour current (Fig. 8).

- Deposition at this site has been complicated by additional controlling factors, such as internal waves, tsunamis, cyclones, mud volcanism, and the Camarinal Sill, etc. (Fig. 8). For these reasons, the Gulf of Cadiz is not an ideal location for developing the contourite facies model with an emphasis on bioturbation (Fig. 9) (Shanmugam, 2016b).
- The term 'contourite' means different things to different people, depending on whose definition one chooses to use. For example, Hollister (1967) would use the term "contourites" for deposits of thermohaline-driven geostrophic contour currents (Fig. 10), whereas Lovell and Stow (1981) would use the term "contourites" for deposits of any kind of bottom currents (Fig. 10). According to Lovell and Stow (1981, 349): "*Contourite: a bed deposited significantly reworked by a current that is persistent in time and space and flows along slope in relatively deep water (certainly below wave base). The water may be fresh or salt; the cause of the current is not necessarily critical to the application of the term*." Clearly, their last phrase "*the cause of the current is not necessarily critical to the application of the term"* has broadened the meaning of the Hollister's (1967) narrow definition of the term contourites. In that broader sense, contourites can be produced by any kind of bottom

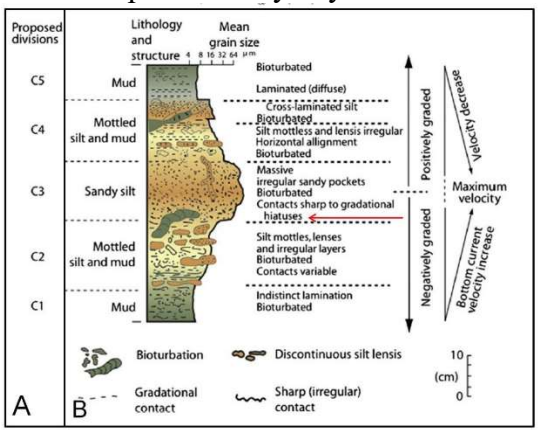

Fig. 9. The contourite facies model showing inverse to normal grading, intense bioturbation, and internal erosional surface (red arrow). Note intense bioturbation is not unique to contourites (Shanmugam, 2016b and 2017). A. Revised contourite facies model with five divisions proposed by Stow and Faugères (2008). B. Original contourite facies model by Faugères et al. (1984). Color version from Rebesco et al. (2014) with additional labels by G. Shanmugam.

current ((e.g., thermohaline-driven, wind-driven, tide-driven, and internal-wave driven). In fact, Stow et al. (2008) explicitly stated that "*Bottom (contour) currents are those currents that operate as part of either the normal thermohaline circulation or wind-driven circulation systems...*" In short, there is no consensus on the meaning of the term 'contourite'. In the absence of a clear definition of contourites, any ichnological analysis of 'contourites' by Rodríguez-Tovar and Hernández-Molina (2018a) is distracting and unnecessary (Shanmugam, 2018a).

It is true that contourites contain bioturbation and trace fossils (Figs. 5 and 6), but that does not mean bioturbation is a characteristic property of contourites. Importantly, bioturbation cannot be used as

a criterion for interpreting deposit of a single process (i.e., contour currents). There are valid reasons for this skepticism:

- Ancient deep-water turbidites (e.g., in the Late Cretaceous Point Loma Formation near San Diego, California) are also extensively bioturbated and even contain the trace fossil *Ophiomorpha* (Nilsen and Abbott, 1979).

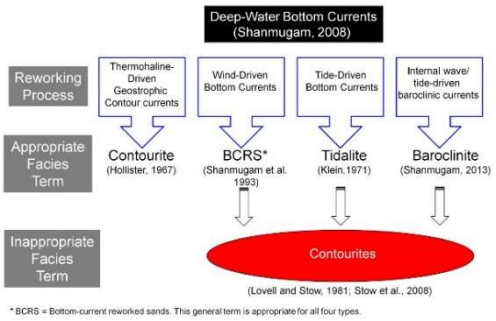

Fig. 10. Four types of bottom currents and their depositional facies. The facies term "contourites" is appropriate only for deposits of thermohaline-driven geostrophic contour currents in deep-water environments, but not for deposits of other three types of bottom currents (i.e., wind, tide, or baroclinic). Note that BCRS represent only sandy lithofacies, but may also be applicable to silty lithofacies. Figure from Shanmugam (2016b), with permission from Elsevier.

- Convincing cases of contourites without bioturbation have been documented in the rock record (Dalrymple and Narbonne, 1996).
- Mulder et al. (2003, 872) cautioned that "*In this case, the hyperpycnite can be mistaken with contourite beds defined by Gonthier, Faugères, and Stow (1984), particularly if bioturbation is intense*."
- Importantly, Hollister (1967, Appendix C, his p. 392) did not even include "bioturbation" as a basic sedimentary feature in the "Sediment Core Logs" of sediments that formed the very foundation for introducing the concept of contourites (his Fig. 1).
- All four types of bottom currents are characterized by traction structures (Fig. 11). The contourite facies model with emphasis on bioturbation (Fig. 9) defies the very first principle of process sedimentology, which is to interpret the fluid mechanics of depositional processes using primary physical sedimentary structures (Sanders, 1963), not bioturbation. The reason is that bioturbation can occur after deposition.

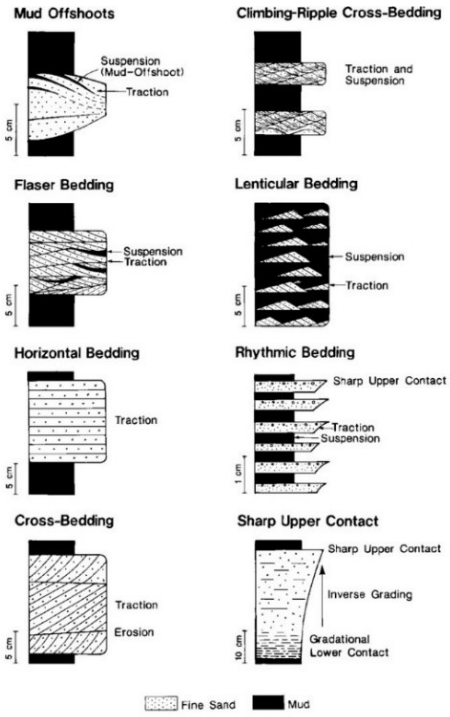

Fig. 11. Summary of traction features interpreted as indicative of deep-water bottom-current reworking by all types of bottom currents. Each feature occurs randomly and should not be considered as part of a vertical facies model. From Shanmugam et al. 1993, with permission from AAPG.

- It is worth pointing out that although Rodríguez-Tovar and Hernández-Molina (2018a) published a review of ichnology of contourites, the same authors (Rodríguez-Tovar and Hernández-Molina (2018b) conceded that "*Nowhere in our manuscript did we*

present bioturbation as an exclusive feature of contourites with respect to other deposits such as turbidites, debrites, etc." Clearly, bioturbation and trace fossils are not diagnostic features of contourites.

In short, bioturbation is of no process sedimentological significance for interpreting ancient deep-water contourite facies.

TURBIDITES

Dott (1963) proposed the most meaningful and practical classification of subaqueous mass-transport processes. It is somewhat analogous to the most widely

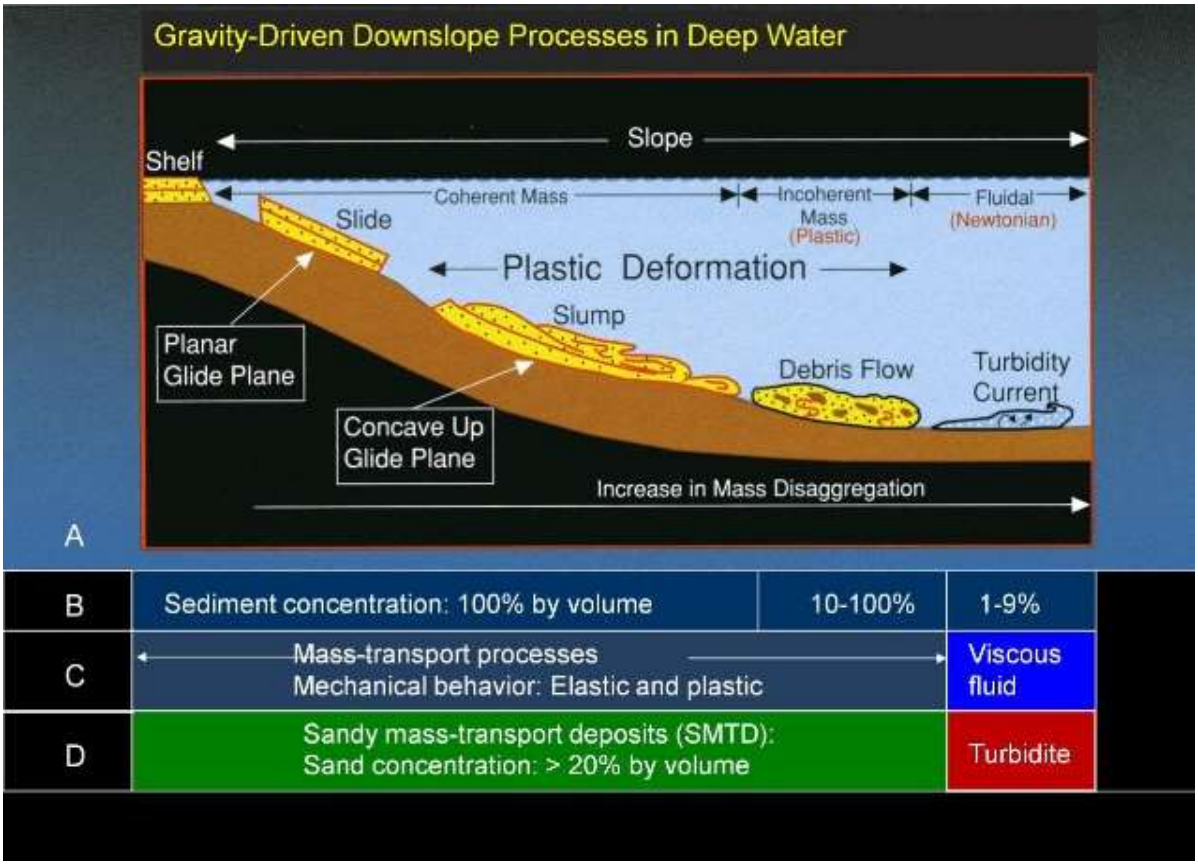

Fig. 12. (A) Schematic diagram showing four common types of gravity-driven downslope processes that transport sediment into deep-marine environments. A slide represents a coherent translational mass transport of a block or strata on a planar glide plane (shear surface) without internal deformation. A slide may be transformed into a slump, which represents a coherent rotational mass transport of a block or strata on a concave-up glide plane (shear surface) with internal deformation. Upon addition of fluid during downslope movement, slumped material may transform into a debris flow, which transports sediment as an incoherent body in which intergranular movements predominate over shear-surface movements. A debris flow behaves as a plastic laminar flow with strength. As fluid content increases in debris flow, the flow may evolve into Newtonian turbidity current. Not all turbidity currents, however, evolve from debris flows. Some turbidity currents may evolve directly from sediment failures. Turbidity currents can develop near the shelf edge, on the slope, or in distal basinal settings. From Shanmugam et al. (1994). (B) Sediment concentration (% by volume) in gravity-driven processes. Slides and slumps are composed entirely of sediment (100% by volume). Debris flows show a range of sediment concentration from 10 to 100% by volume. Note that turbidity currents are low in sediment concentration (<9% by volume, after Bagnold, 1962); implying low-density flows. These values are based on published data (see Shanmugam, 2000, his Figure 4). (C) Based on mechanical behavior of gravity-driven downslope processes, mass-transport processes include slide, slump, and debris flow, but not turbidity currents (Dott, 1963). (D) The prefix "sandy" is used for mass-transport deposits (SMTDs) that have grain (>0.06 mm: sand and gravel) concentration value equal to or above 20% by volume. The 20% value is adopted from the original field classification of sedimentary rocks by Krynine (1948). Modified after Shanmugam (2012).

accepted classification of subaerial mass-transport processes by Varnes (1958). The importance of Dott's (1963) classification is that mass-transport processes do not include turbidity currents (Fig. 12C). The underpinning principle of Dott's (1963) classification is the separation of solid from

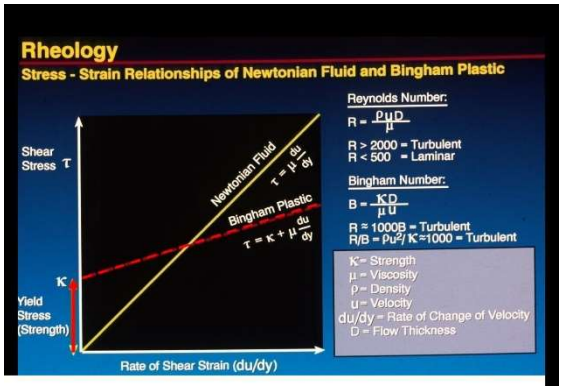

Fig. 13. Graph showing rheology (stress–strain relationships) of Newtonian fluids and Bingham plastics. Note that the fundamental rheological difference between debris flows (Bingham plastics) and turbidity currents (Newtonian fluids) is that debris flows exhibit strength, whereas turbidity currents do not. Reynolds number is used for determining whether a flow is turbulent (turbidity current) or laminar (debris flow) in state. Compiled from several sources (Dott, 1963; Enos, 1977; Pierson and Costa, 1987; Phillips and Davies, 1991; Middleton and Wilcock, 1994). From Shanmugam (1997).

fluid mode of transport based on sediment concentration. In the solid (elastic and plastic) mode of transport, high sediment concentration is the norm (10-100% by volume, Fig. 12B). Mass-transport mechanisms are characterized by solid blocks or aggregate of particles (mass). In contrast, individual particles are held in suspension by fluid turbulence in turbidity currents (Dott, 1963; Sanders, 1965). Turbidity currents are characterized by low sediment concentration of less than 9% by volume, which was proposed by Bagnold (1962) (Fig. 12B). In other words, turbidity currents are innately low in flow density.

In this article, the focus is on debris flows and turbidity currents because of their sedimentological importance. These two processes are distinguished from one another on the basis of fluid rheology and flow state. The rheology of fluids can be expressed as a relationship between applied shear stress and rate of shear strain (Fig. 13). Newtonian fluids (i.e., fluids with no inherent strength), like water, will begin to deform the moment shear stress is applied, and the deformation is linear. In contrast, some naturally occurring materials (i.e., fluids with strength) will not deform until their yield stress has been exceeded (Fig. 13); once their yield stress is exceeded, deformation is linear. Such materials (e.g., wet concrete) with strength are considered to be Bingham plastics (Fig. 13). For flows that exhibit plastic rheology, the term plastic flow is appropriate. Using rheology as the basis, deep-water sediment flows are divided into two broad groups, namely, (1) Newtonian flows that represent turbidity currents and (2) plastic flows that represent debris flows.

A turbidity current is a sediment flow with Newtonian rheology and

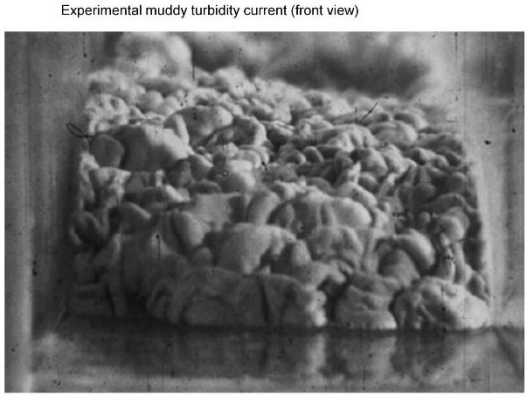

Fig. 14. Photograph of front view of experimental turbidity current showing flow turbulence. Photo from experiments conducted by M.L. Natland, and courtesy of G.C. Brown. Published in Shanmugam (2012) with permission.

turbulent state (Fig. 14) in which sediment is supported by turbulence and from which deposition occurs through suspension settling (Dott, 1963; Sanders, 1965; Middleton and Hampton, 1973; Shanmugam, 1996, 2006). Turbidity currents exhibit unsteady and non-uniform flow behavior (Fig. 15), and they are surge-

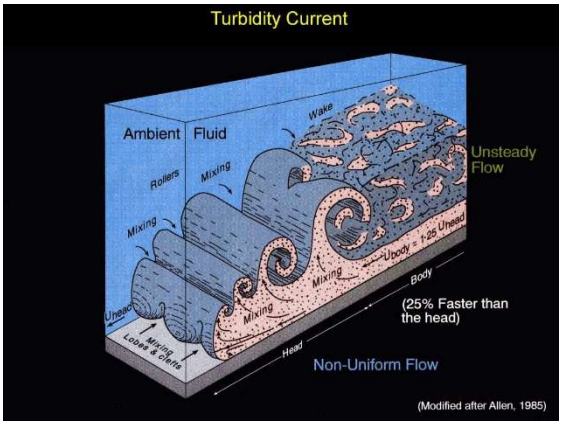

Fig. 15. Schematic illustration showing the leading head portion of an unsteady, nonuniform, and turbulent turbidity current. Due to turbulent mixing, turbidity currents invariably entrain ambient fluid (seawater) at their head regions. Modified from Allen (1985).

type waning flows. As they flow downslope, turbidity currents invariably entrain ambient fluid (sea water) in their frontal head portion due to turbulent mixing (Allen, 1985). With increasing fluid content, plastic debris flows may tend to become Newtonian turbidity currents (Fig. 12A). However, not all turbidity currents evolve from debris flows. Some turbidity currents may evolve directly from sediment failures. Although turbidity currents may constitute a distal end member in basinal areas, they can occur in any part of the system (i.e., shelf edge, slope, and basin).

Turbidity currents cannot transport gravel and coarse-grained sand in suspension because they do not possess the strength like debris flows. General characteristics of turbidites are:

- Fine-grained sand to mud Flute casts; however, flute casts are not unique to turbidites (see Klein, 1966; Shanmugam, 2002a)
- Normal grading (core and outcrop) (Fig. 16).
- Sharp or erosional basal contact (core and outcrop) (Fig. 16)
- Gradational upper contact (core and outcrop) (Fig. 16)
- Thin layers, commonly centimeters in thickness (core and outcrop)
- Sheet-like geometry in basinal settings (outcrop)
- Lenticular geometry may develop in channel-fill settings.

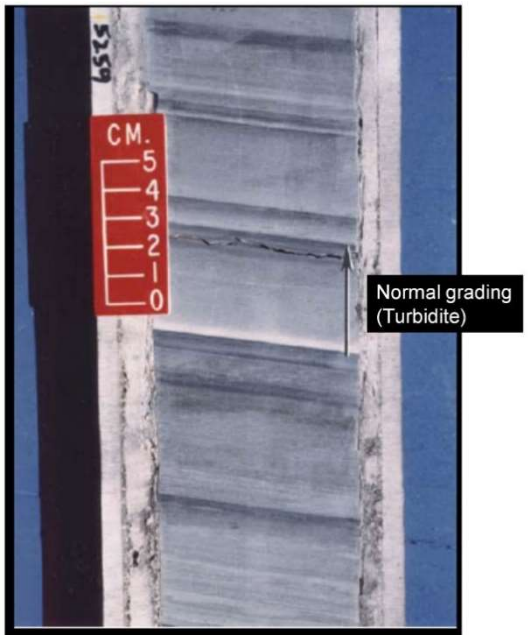

Fig. 16. Core photograph showing turbidite units with sharp basal contact, normal grading, and gradational upper contact. Arrow marks a normally graded unit with fine-grained sand at bottom (light gray) grading into clay (dark gray) near to Note that these thin-bedded units cannot be resolved on seismic data. Zafiro Field, Pliocene, Equatorial Guinea. From Shanmugam (2006) with permission from Elsevier.

In the Maritime Alps, Phillips et al. (2011) described the ichnology of the Grès d'Annot Basin, SE France in detail for the first time. In this case, deep marine palaeo environments from basin slope to basin floor settings are preserved. The Grès d'Annot Formation is a sand-rich, thick-bedded, and coarse-grained turbidite succession. Thick-bedded and channel sandstones contain low diversity trace fossil assemblages dominated by Ophiomorpha (Fig.17). Ophiomorpha in the Grès d'Annot Basin is inferred to have been produced by organisms mostly deposit feeding on buried organic-rich material during inter-turbidite intervals. *Ophiomorpha rudis* is the most prominent trace fossil found in the Grès d'Annot Basin and dominates the

ichnofabrics in all locations within the basin. The deep-burrowing ability of the Ophiomorpha animal is considered to be an adaptation for exploiting buried organic nutrients found in inter-turbidite mudstones (Fig. 18).

Turbidite facies models

Conventionally, coarse-grained turbidites are considered to be deposits of high-density turbidity currents (Lowe, 1982). The problem is that high-density turbidity currents are nothing more than sandy debris flows in terms of fluid rheology and low state (Shanmugam, 1996, 2016c). Amid this controversy, ascribing trace fossils to coarse-grained or high-density turbidites in the Annot Sandstone (Figs. 17, 18) is problematic. Specific issues are:

1. Turbidity currents are inherently low in sediment concentration or low in flow density (Fig. 19A), According to Bagnold (1962), typical turbidity currents can function as truly turbulent suspensions only when their sediment concentration by volume is below 9% or C < 9% (Fig. 19A). Therefore, true high-density turbidity currents cannot exist in nature (Shanmugam, 1996, 2000).
2. There is no agreement on the density value that separates "low-

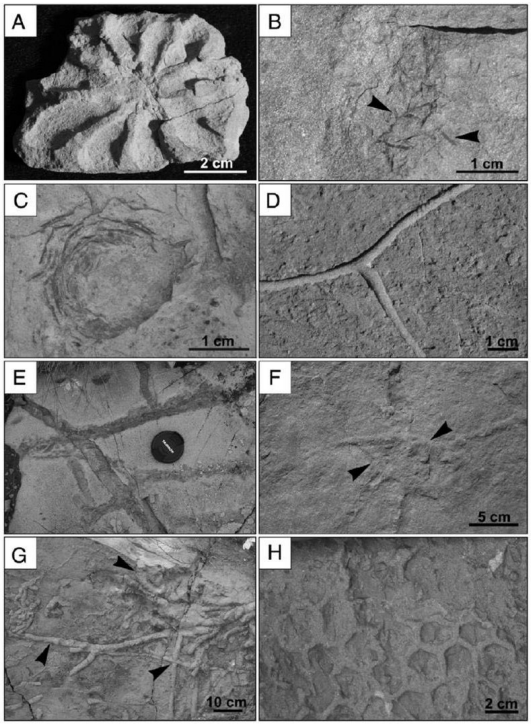

Fig. 17. Field images of documented trace fossils. A) *Asterosoma radicifo*rme found on top of a thin-bedded turbidite. Braux. B) Branched *Chondrites* is (arrowed) within a very fine-grained sandstone turbidite. Braux. C) Shell-lined *Diopatrichnus* from the uppermost Marnes Bleues Formation. Argenton. D) *Ophiomorpha annulata* on the sole of a thin-bedded sandstone turbidite. Montagne de Chalufy. E*) Ophiomorpha ?nodosa* on top of a coarse-grained sandstone turbidite. *Col de la Cayolle*. Lens cap is 5 cm wide. F) Knotted *Ophiomorpha rudis* on top of an inter-turbidite claystone. Baisse de l'Aiguille. G) Numerous *Ophiomorpha rudis* (arrowed) on the sole of a sandstone turbidite, Argenton. H) *Paleodictyon majus* on the sole of a thin-bedded, very fine-grained sandstone turbidite. *Col de la Cayolle*. From Phillips et al. (2011).

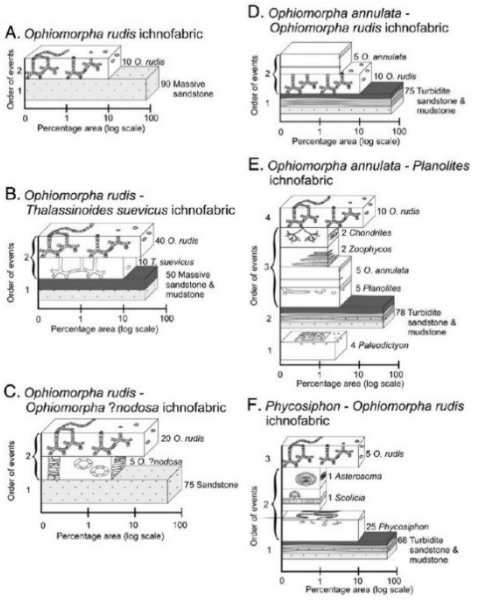

Fig. 18. Ichnofabric constituent diagrams for three ichnofabric associations and six ichnofabrics documented. The vertical axis indicates the order of events starting with either preturbidite ichnotaxa or turbidite deposition followed by colonization by post-depositional ichnotaxa. Numbers associated with each event indicate the percentage (by area) of the ichnofabric constituted by each event. From Phillips et al., (2011).

density" from "high-density" turbidity currents (Fig. 19A).

3. A reexamination of the Annot Sandstone in the Peira Cava area in SE France, Maritime Alps, which served as the type locality for the 'Bouma Sequence', suggests deposition from sandy debris flows (Fig. 20), not classic turbidity currents (see Shanmugam, 1997 and 2002a).
4. Flume experiments have revealed that the so-called 'high-density turbidity currents' are indeed composed of a basal laminar layer, typical of debris flows (Fig. 19B), not turbulent turbidity currents. This experiment also provided evidence for deposition of floating

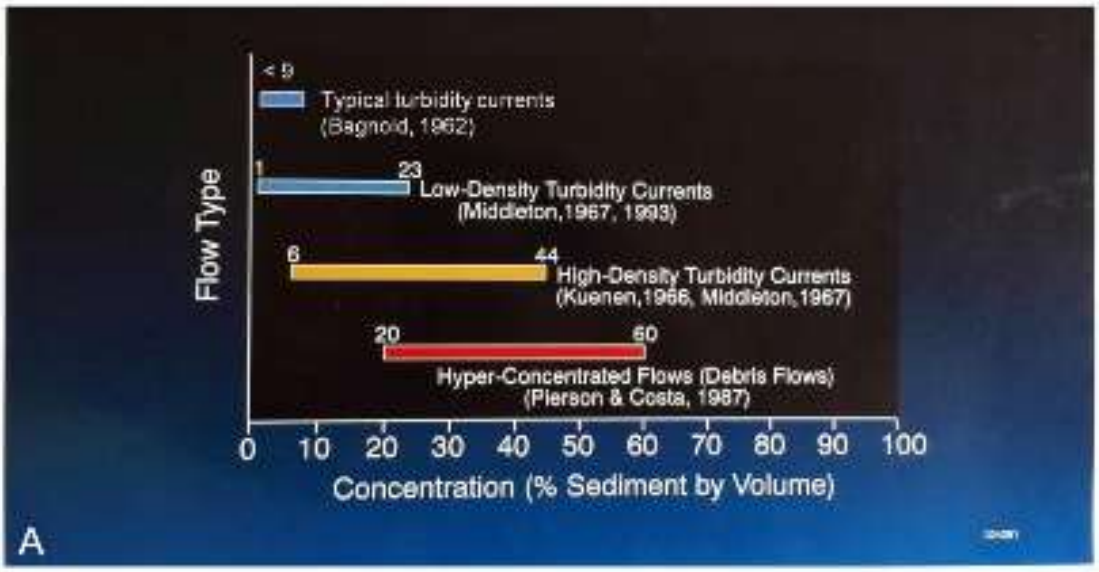

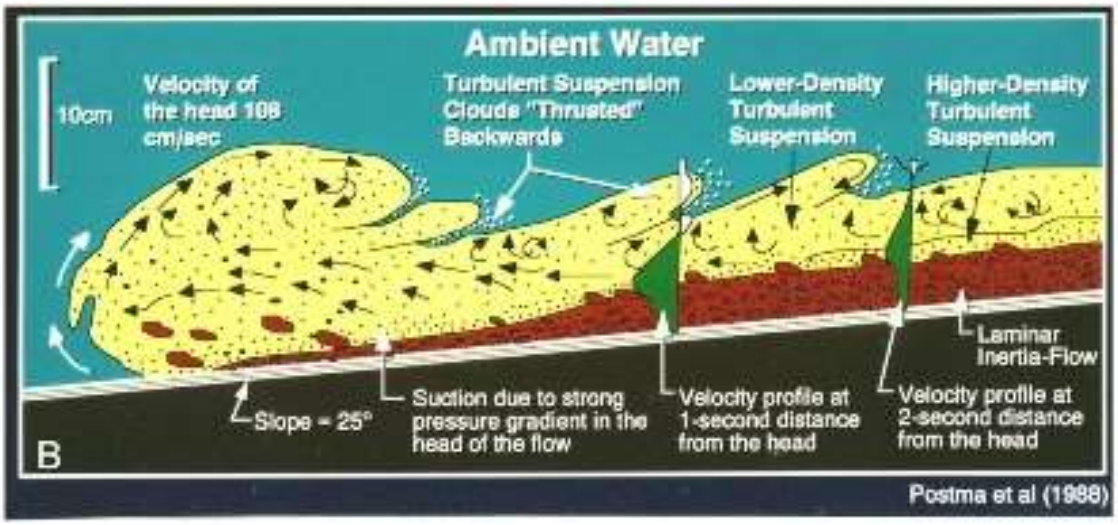

Fig. 19. A-Plot of sediment concentration for different flow types. Note that a typical turbidity current can exist only in sediment concentration less than 9% by volume (Bagnold, 1962). Note that "high-density turbidity currents" are nothing but "sandy debris flows" (Shanmugam, 1996). Modified after Shanmugam (1996). Reproduced with permission from SEPM; B-Experimental stratified flows with a basal laminar-inertia flow and an upper (turbulent) turbidity current that have been termed as "high-density turbidity currents." Figure from Postma et al. (1988). Publication: Sedimentary Geology. With permission from Elsevier.

clasts (Postma et al., 1988), common in debris flows

5. No one has ever documented empirical data on active 'gravelly or sandy turbidity currents' in modern oceans using vertical sediment concentration profiles and grain-size measurements.
6. No one has ever documented the vertical facies model showing the R1, R2, R3, S1, S2, and S3 divisions of the Lowe (1982) sequence and the Ta, Tb, Tc, Td, and Te divisions of the Bouma (1962) sequence in ascending order (Fig. 21A) in modern deep-sea sediments.

Given these uncertainties concerning the fundamentals of coarse-grained turbidites, the link between bioturbation and high-density turbidity currents is incongruous. In short, bioturbation is of no process sedimentological significance for interpreting ancient deep-water turbidite facies, be it low-density or high-density types..

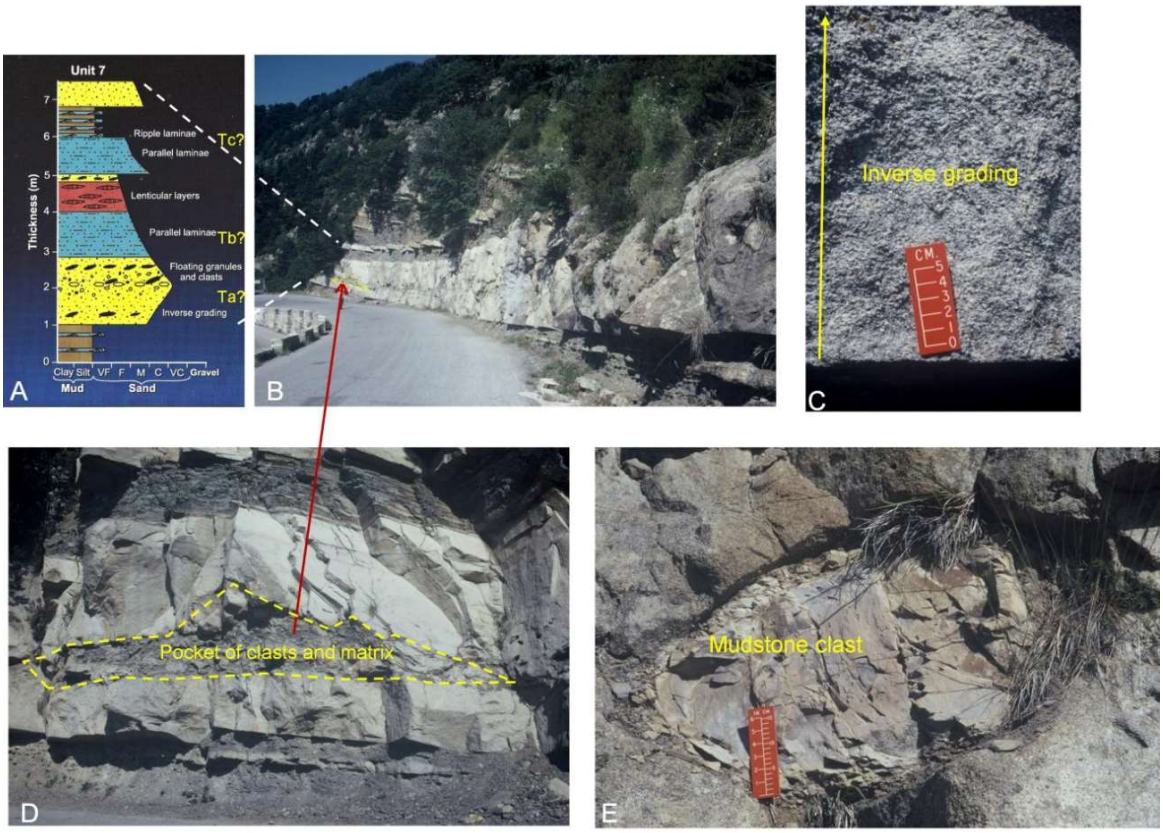

Fig. 20. A-Sedimentological log of amalgamated sandstone Unit 7 showing basal inverse grading overlain by an interval of complex normal grading with floating granules and mudstone clasts, parallel laminae, and lenticular layers. Note sudden increase in grain size at 5m. Note conventional description using Bouma notations (Ta, Tb, and Tc); B-Outcrop photograph of Unit 7 showing sheet-like geometry; C-Outcrop photograph of Unit 7 showing basal inversely graded interval in coarse- to granule-grade sandstone; D-Outcrop photograph of a pocket of clasts and matrix in the middle of the unit. Arrow shows stratigraphic position of photo; E-Outcrop photograph of Unit 7 showing a floating mudstone clast in the middle of the unit. Annot Sandstone (Eocenee-Oligocene), Peira Cava area, French Maritime Alps, SE France. Figures compiled from Shanmugam (2002a). Publication: Earth-Science Reviews. With permission from Elsevier.

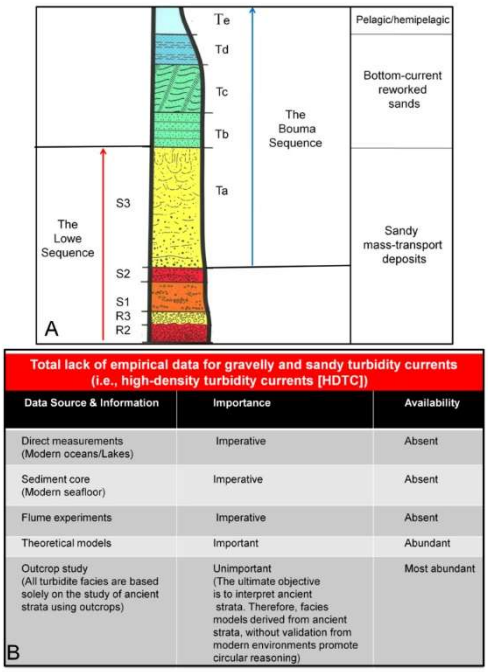

Total lack of empirical data for gravelly and sandy turbidity currents (i.e., high-density turbidity currents [HDTC])

Data Source & Information	Importance	Availability
Direct measurements (Modern oceans/Lakes)	Imperative	Absent
Sediment core (Modern seafloor)	Imperative	Absent
Flume experiments	Imperative	Absent
Theoretical models	Important	Abundant
Outcrop study (All turbidite facies are based solely on the study of ancient strata using outcrops)	Unimportant (The ultimate objective is to interpret ancient strata. Therefore, facies models derived from ancient strata, without validation from modern environments promote circular reasoning)	Most abundant

B

Fig. 21. A. Schematic diagram showing an ideal turbidite bed with nine turbidite divisions by combining the five divisions of the "Bouma Sequence" (Bouma, 1962) and the five divisions of the "Lowe Sequence" of high-density turbidites (Lowe, 1982). According to Lowe (1982), S3=Ta. On the right-hand column, interpretations of these divisions are shown. Figure from Shanmugam (2012). B. Summary diagram revealing the total lack of empirical data for high-density turbidity currents (see Shanmugam, 2012 for details).

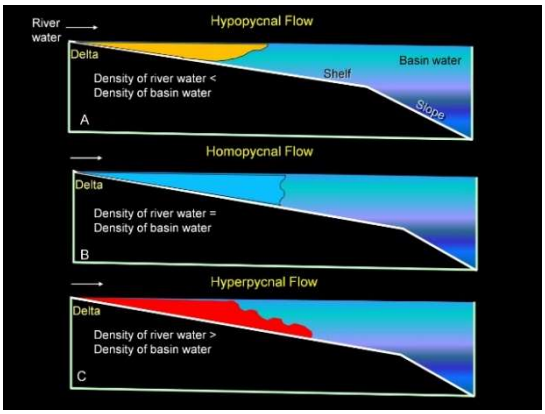

Fig. 22. Three types of density plumes based on concepts of Bates (1953). A. Hypopycnal plume in which density of river water is less than density of basin water. B. Homopycnal plume in which density of river water is equal to density of basin water. C. Hyperpycnal plume in which density of river water is greater than density of basin water. Figure From Shanmugam (2012).

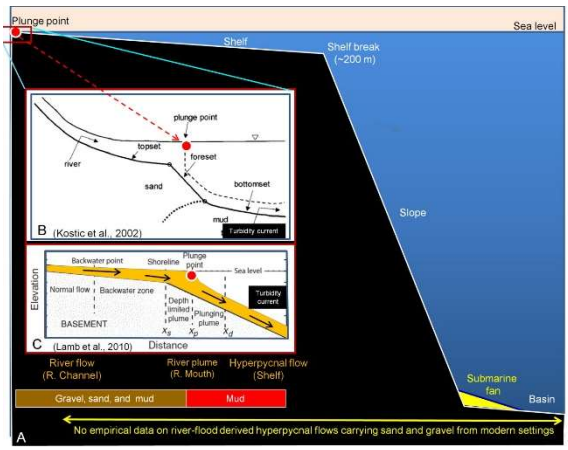

Fig. 23. Continental margin and flume experiments. A Conceptual diagram of a continental margin showing relative positions of plunge point (red filled circle) at river mouth and submarine fan at base-of-slope. Average shelf width = 80 km. Maximum shelf width = 1,500 km; B Schematic diagram, based on flume experiments conducted using fresh water as standing body, showing transformation of river current into turbidity current at plunge point (red filled circle). Note that this experiment using fresh water is applicable to fresh water lakes, but not to marine settings (sea or ocean). From Kostic et al. (2002) with additional labels; C Schematic diagram with backwater zone showing transformation of river plume into turbidity currents at plunge point (red filled circle). Note the close similarity between B and C on the initiation of turbidity currents at plunge point. In this study, the term "hyperpycnal flow" is used for flows seaward of the plunge point, instead of turbidity current. From Lamb et al. (2010) with additional symbols. From Shanmugam (2018b). Springer, Open Access.

Hyperpycnites

The term "hyperpycnite" (*i.e.*, deposits of hyperpycnal flows) was first introduced by Mulder *et al*. (2002) in an academic debate with me (Shanmugam, 2002b) on the origin of inverse grading by hyperpycnal flows. The importance of bioturbation in hyperpycnites has been discussed by several authors (Mulder et al., 2003; Buatois et al., 2011, among others). A brief review of hyperpycnites in terms of our understanding is in order.

Sedimentologic, oceanographic, and hydraulic engineering publications on hyperpycnal flows (Fig. 22) claim that (1) river flows transform into turbidity currents

Fig. 24. Dissipating plumes, Rio de la Plata Estuary, South America. From Shanmugam (2018c). Elsevier.

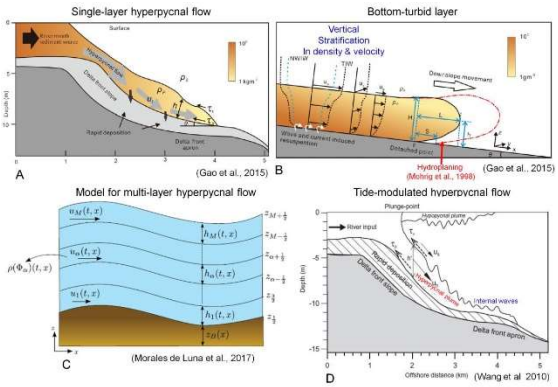

Fig. 25 Variable types of hyperpycnal flows. A Single-layer hyperpycnal flow, Yellow River, China. Color concentration = Suspended sediment concentration; h = Flow thickness; τt = Upper surface; τb = Bed shear stress. From Gao et al. (2015); B Bottom turbid layer with density and velocity stratification (i.e., debris flow with hydroplaning, red arrow added in this article, see text), Yellow River, China. Uw=Wave orbital velocity; Uc = Along shelf current magnitude; Ug = Velocity of gravity current; NWIW= Normal wind-induced wave velocity; TIW= Typhoon-induced wave. The red line represents the downslope variation trend of the bottom-turbid layer. From Gao et al. (2015) with additional labels; C Multi-layer hyperpycnal flow in numerical modeling (Morales de Luna et al. 2017). Note that multi-layer numerical modeling was also applied to hypopycnal flows. h = Height of a fluid layer; u = Velocity; ϕ = Particle concentration; ρ = Density. See Morales de Luna et al. (2017) for details of various parameters and related equations; D Tide-modulated hyperpycnal flow, Yellow River (Wang et al. 2010; modified after Wright et al. 1988), with permission from John Wiley and Sons. Color labels by G. Shanmugam. Note internal waves. Internal waves occur only along pycnoclines (Shanmugam 2013), but there is no indication of pycnoclines in this diagram.

at plunge points near the shoreline (Fig. 23B)., (2) hyperpycnal flows have the power to erode the seafloor and cause submarine canyons (Lamb et al. 2010), and, (3) hyperpycnal flows are efficient in transporting sand across the shelf and can deliver sediments into the deep sea for developing submarine fans (Steel et al. 2016; Warrick et al. 2013; Zavala and Arcuri 2016) (Fig. 23A).

Importantly, these claims do have economic implications for the petroleum industry for predicting sandy reservoirs in deep-water petroleum exploration and production (Yang et al., 2017). However, these claims are based strictly on experimental or theoretical basis, without the supporting empirical data from modern depositional systems. In resolving this issue, Shanmugam (2018b, c) rigorously evaluated the merits of these claims by a global evaluation of density plumes that include hyperpycnal flows, based on 45 case studies that include 21 major rivers (e.g., Yellow River, Yangtze River, Copper River, Hugli River (Ganges), Guadalquivir River, Río de la Plata Estuary (Fig. 24), Zambezi River, among others). This global study suggests a complex variability in nature. Multiple flow types have been proposed (Fig. 25).

Fig. 26. Summary diagram showing complex natural variability of plumes in terms of their environmental settings, their composition, their source, their external control, and types. This compilation of factors should be considered preliminary. For example, gas hydrate is included in more than one category. Modified after Shanmugam (2018b). Springer, Open Access.

For example, there are at least 16 types of hyperpycnal flows (e.g., density flow, underflow, high-density hyperpycnal plume, high-turbid mass flow, tide-modulated hyperpycnal flow, cyclone-induced hyperpycnal turbidity current, multi-layer hyperpycnal flows, etc.), without an underpinning principle of fluid dynamics (Shanmugam, 2018b).

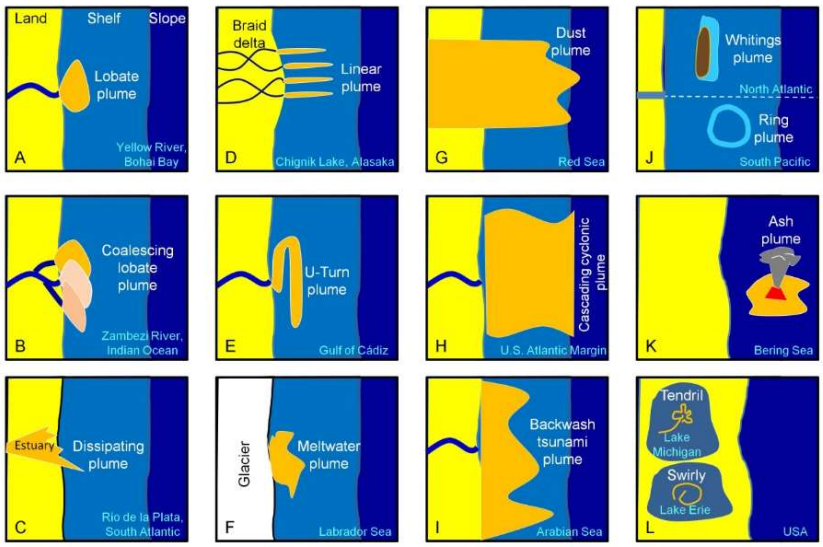

Fig. **27.** Summary diagram showing 14 general types of plumes that include 12 marine examples and two lacustrine examples. From (Shanmugam, 2018b). Springer, Open Access.

A summary diagram (Fig. 26) of real-world examples show that density plumes (1) occur in six different environments (i.e., marine, lacustrine, estuarine, lagoon, bay, and reef); (2) are composed of six different compositional materials (e.g., siliciclastic, calciclastic, planktonic, etc.); (3) derive material from 11 different sources (e.g., river flood, tidal estuary, subglacial, etc.); (4) are subjected to 18 different external controls (e.g., tidal shear fronts, ocean currents,

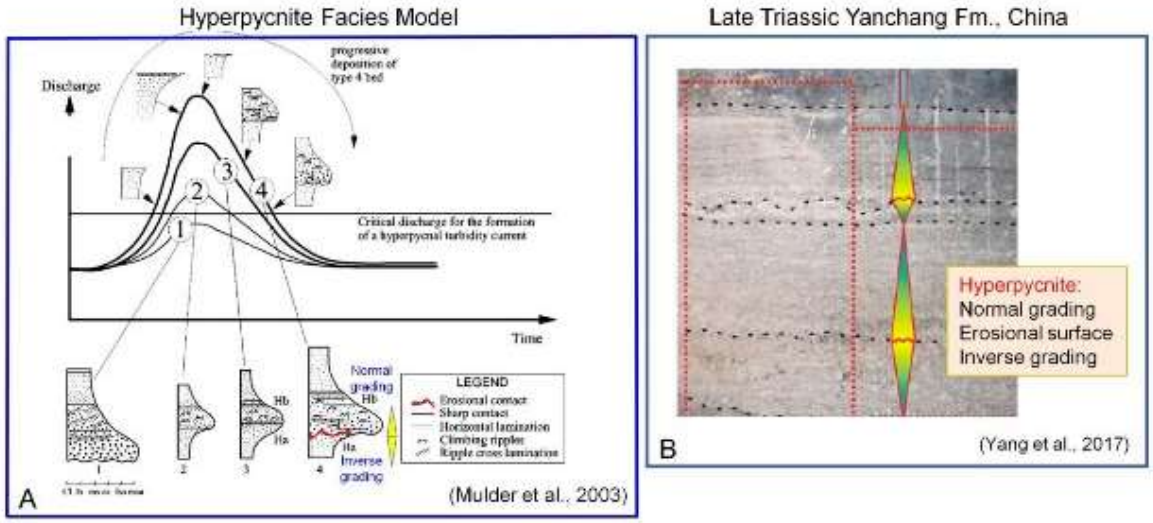

Fig. 28. A- Hyperpycnite facies model showing inverse to normal grading with erosional contact in the middle. In example 4 at the bottom, yellow triangles showing normal and inverse gradings are inserted by G. Shanmugam. From Mulder *et al.* (2003) with permission from Elsevier. B - An ancient example from China interpreted as a hyperpycnite showing inverse to normal grading with an internal erosional surace. The presence of an internal erosional surface within a single depositional unit by a single flow is antithetical to basic principles of stratigraphy and sedimentation (Krumbein and Sloss, 1963). The reason is that the presence of an internal erosional surface suggests that the lower inverse grading and the upper normal grading divisions could be deposited by two different events, separated by a hiatus. From Yang *et al.* (2017) with additional labels by G. Shanmugam.

cyclones, tsunamis, etc.); and, (5) exhibit 24 configurations (e.g., lobate, coalescing, linear, swirly, U-Turn, anastomosing, etc.) (Fig.26). These plumes do not transport sand from shoreline to the deep sea. The exceptions are cyclone, tsunamis, and eolian dust (Fig. 27).

In summary, available data do not support the notion that river-induced hyperpycnal flows transport sand across the shelf and deliver sand into the deep sea for developing submarine fans and related petroleum reservoirs.

Like turbidite and contourite facies models, hyperpycnite facies model (Fig. 28) suffers from numerous uncertainties (see Shanmugam, 2018b). Because there is no documented link between fluid mechanics of hyperpycnal flows and bioturbation, the presence of ichnological signatures in hyperpycnites is of no consequence from a depositional process viewpoint.

Concluding Remarks

Deep-water depositional facies are highly complex in their sedimentary features. This is because of a combination of factors, such as soil mechanics, fluid mechanics, elements of physical oceanography, etc., which influence deposition. Deep-water settings are prone to develop hybrid flows and, importantly, the link between flow mechanics and ichnology is an unknown entity yet. Amid these challenges, the promotion of ichnological signatures in a specific deep-water facies is of no depositional relevance.

Acknowledgements:

The late George Devries Klein (1933-2018) served as my mentor and friend during the past 40 years. I thank Prof. G. M. Bhat, Managing Editor of JIAS, for organizing this special issue in celebrating the contributions of George Klein. I wish to thank the journal reviewer Nallappa Reddy for a thorough review. I am grateful to my wife Jean for her general comments.

References

Ager, D. V. (1973). The Nature of the Stratigraphic Record. MacMillan, New York, 114.

Allen, J.R.L. (1985). Loose-boundary hydraulics and fluid mechanics: Selected advances since 1961 In: J. Brenchley , J. Williams (eds.). Sedimentology: recent developments and applied aspects 1985 Published for the Geological Society by Blackwell Scientific Publications Oxford, 7-28

Bagnold, R.A. (1962). Auto-suspension of transported sediment. Philosophical Transactions of the Royal Society of London. Series A, Mathematical and Physical Sciences 265, 315-319.

Bates, C.C., (1953). Rational theory of delta formation. AAPG Bulletin, 37, 2119-2162.

Bouma, A.H., (1962). Sedimentology of Some Flysch Deposits, A graphic Approach to Facies Interpretation. Elsevier, Amsterdam, 168.

Buatois, L. A., Saccavino, L. L. and Zavala, C. (2011). Ichnologic signatures of hyperpycnal flow deposits in Cretaceous river-dominated deltas, Austral Basin, southern Argentina. In: . Slatt, R. M. and Zavala, C. (Eds.), Sediment transfer from shelf to deep water—Revisiting the delivery system. AAPG Studies in Geology, 61, 153– 170.

Dalrymple, R.W., and Narbonne, G.M. (1996). Continental slope sedimentation in the Sheepbed Formation (Neoproterozoic, Windermere Supergroup), Mackenzie Mountains, N.W.T. Cananadian Journal of Earth Science, 33, 848-862.

Dott, R.H., Jr. (1963). Dynamics of subaqueous gravity depositional processes. AAPG Bulletin, 47, 104–128.

Embley, R.W. (1980|. The role of mass transport in the distribution and character of deep-ocean sediments with special reference to the North Atlantic. Marine Geology, 38, 23–50.

Enos, P. (1977). Flow regimes in debris flow. Sedimentology, 24, 133-142.

Faugères, J.-C., Gonthier, E., and Stow, D.A.V. (1984). Contourite drift moulded by deep Mediterranean outflow. Geology, 12, 296–300.

Flood, R.D. and Hollister, C.D. (1974). Current-controlled topography on the continental margin off the eastern United States. in: Burke, C.A. and Drake C L (eds.). The Geology of Continental Margins. New York, Springer-Verlag, 197–205.

Fortuin, A.R., and Dabrio, C.J. (2008). Evidence for Late Messinian seismites, Nijar Basin, south-east Spain. Sedimentology, 55, 1595-1622.

Fossati, M., and Piedra-Cueva, I. (2013). A 3D hydrodynamic numerical model of the Río de la Plata and Montevideos coastal zone. Applied Mathematical Modelling, 37, 1310–1332.

Fossati, M., Cayocca, F., and Piedra-Cueva, I. 2014. Fine sediment dynamics in the Río de la Plata. Advances in Geosciences, 39, 75–80.

Gao, S., Wang, D., Yang, Y., Zhou, L., Zhao, Y., Gao, W., Han, Z., Yu, Q. and Li, G. (2015). Holocene sedimentary systems on a broad continental shelf with abundant river input: Process–product relationships. In: D. Clift, J. Harff, J. Wu, and Y. Qui, (eds.), River-dominated shelf sediments of east Asian seas. London, Geological Society, Special Publications, 429, 223–259..

Gonthier, E.G., Faugères, J.-C., and Stow, D.A.V. (1984). Contourite facies of the Faro Drift, Gulf of Cadiz. In: Stow, D.A.V. and Piper, D.J.W. (eds.), Fine-Grained Sediments: Deep-Water Processes and Facies, Geological Society of London Special Publication 15, Geological Society of London, 275-292.

Greene, T.J., Gingras, M.K., Gordon, G., and McKeel, D.R. (2012). The significance of deep-water cryptic bioturbation in slope-channel massive sand deposits of the lower Rio Dell Formation, Eel River basin, California. Marine and Petroleum Geology, 29, 152-174.

Heezen, B.C., Hollister, C.D. and Ruddiman, W.F., (1966). Shaping of the continental rise by deep geostrophic contour currents. Science, 152, 502-508.

Hollister, C.D. (1967). Sediment distribution and deep circulation in the western North Atlantic, Ph.D. dissertation, Columbia University, New York., 467.

Klein, G. D. (1971). A sedimentary model for determining paleotidal range. GSA Bulletin, 82, 2585-2592.

Knaust, D. (2012). Methodology and techniques. In: Knaust, D., Bromley, R.G. (Eds.), Trace Fossils as Indicators of Sedimentary Environments. Developments in Sedimentology, 64. 245–271.

Kostic, S., Parker, G. and Marr. J. G. (2002). Role of turbidity currents in setting the foreset slope of clinoforms prograding into standing fresh water. Journal of Sedimentary Research, 72 (3), 353–362.

Krumbein, W.C., and Sloss, L.L. (1963), Stratigraphy and Sedimentation, 2nd Edition. W.H. Freeman and Company, San Francisco, 660.

Krynine, D. (1948). The megascopic study and field classification of sedimentary rocks. The Journal of Geology, 56, 130-165.

Lamb, M.,B. McElroy, B., Kopriva, J., Shaw, and Mohrig, D. (2010). Linking riverflood dynamics to hyperpycnal-plume deposits: experiments, theory, and geological implications. GSA Bulletin, 122, 1389–1400.

Lovell, J.B., and Stow, D.A.V. (1981). Identification of ancient sandy contourites. Geology, 9, 347-349

Lowe, D.R. (1982). Sediment gravity flows, II. depositional models with special reference to the deposits of high-density turbidity currents. Journal of Sedimentary Petrology, 52, 279–297.

MacEachern, J.A., Pemberton, S.G., Gingras, M.K., and Bann, K.L. (2010). Ichnology and facies models. In: James, N. and Dalrymple, R.W. (eds.), Facies Models 4. Geol. Ass. Can., St. John's, Geotext 6. 19–58.

Middleton, G.V., and Hampton, M.A., (1973). Sediment gravity flows: Mechanics of

flow and deposition. In: Middleton, G.V., and Bouma, A.H., (eds). Turbidites and Deep-Water Sedimentation. Los Angeles, California: Pacific section SEPM, 1-38.

Middleton, G.V., and Wilcock, R., (1994). Mechanics in the Earth and Environmental Sciences. Cambridge, Cambridge University Press, 459.

Mohrig, D., Whipple, K.X., Hondzo, M., Ellis, C., and Parker, G. (1998). Hydroplaning of subaqueous debris flows. GSA Bulletin, 110, 387-394.

Morales de Luna, T., Fernández Nieto, E.D. and Castro Díaz, M.J. (2017). Derivation of a multilayer approach to model suspended sediment transport: Application to hyperpycnal and hypopycnal plumes. Communications in Computational Physics, 22 (5): 1439–1485.

Mulder, T., Migeon, S., Savoye, B. and Faugères, J.-C. (2002). Reply to discussion by Shanmugam on Mulder et al. (2001, Geo-Marine Letters, 21, 86–93) Inversely graded turbidite sequences in the deep Mediterranean. A record of deposits from flood-generated turbidity currents? Geo-Marine Letters, 22, 112–120.

Mulder, T., Syvitski, J.M., Migeon, S., Faugeres, J.-C., and Savoye, B., (2003). Marine hyperpycnal flows: initiation, behavior and related deposits: a review. Marine and Petroleum Geology, 20, 861-882.

Murray, J., Renard, A.F. (1891). Report on deep-sea deposits based on specimens collected during the voyage of H.M.S. Challenger in the years 1872–1876. Government Printer, Challenger Reports, London, 525.

Mutti, E. (1992). Turbidite Sandstones. Agip Special Publication, Milan, Italy, 275.

Nilsen, T. H., and Abbott, L., (1979). Introduction. In: Nilsen TH, Arthur MA (eds) Upper Cretaceous deep-sea fan deposits, San Diego. Geol Soc Am Annu Meet, San Diego, CA, Fieldtrip 11, 137–166.

Phillips, C.J., and Davies, T.R.H., (1991). Determining rheological parameters of debris flow material. Geomorphology, 4, 101-110.

Phillips, C., Mcllroy, D. and Elliott, T. (2011). Ichnological characterization of Eocene/Oligocene turbidites from the Grès d'Annot Basin, French Alps, SE France. Palaeogeography, Palaeoclimatology, Palaeoecology, 300, 67–83.

Pierson, T.C., and Costa, J.E., (1987). Arheologic classification of subaerial sediment-water flows. In: Costa, J.E., Wieczorek, G.F., (eds.), Debris Flows/Avalanches, Process, Recognition, and Mitigation, vol. VII. Boulder, CO, GSA Reviews in Engineering Geology, 1-12.

Postma, G., Nemec, W., and Kleinspehn, K.L., (1988). Large floating clasts in turbidites, a mechanism for their emplacement. Sedimentary Geology, 58, 47-61.

Rebesco, M., Hernández-Molina, F. J. Van Rooij, D., and Wåhlin, A., (2014). Contourites and associated sediments controlled by deep-water circulation processes: State-of-the-art and future considerations. Marine Geology, 352, 111–154.

Rodríguez-Tovar, F. J., Hernández-Molina, F. J. (2018a). Ichnological analysis of contourites: Past, present and future. Earth-Science Reviews, 182, 28–41

Rodríguez-Tovar, F. J., Hernández-Molina, F. J. (2018b). Reply to Comment on "Ichnological analysis of contourites: Past, present and future" by Francisco J. Rodríguez-Tovar and F. Javier Hernandez-Molina [Earth-Science Reviews, 182 (2018), 28–41]. Earth-Science Reviews, 184, 50-51.

Sanders, J.E. (1965). Primary sedimentary structures formed by turbidity currents and related resedimentation mechanisms. In: Middleton, G.V. (ed.), Primary Sedimentary Structures and Their Hydrodynamic Interpretation, 12. SEPM Special Publication, Tulsa, OK, 192-219.

Seilacher, A. (1964). Sedimentological classification and nomenclature of trace fossils. Sedimentology, 3, 253–256.

Shanmugam, G. (1996). High-density turbidity currents, are they sandy debris flows? Journal of Sedimentary Research, 66, 2-10.

Shanmugam, G. (1997). The Bouma sequence and the turbidite mind set. Earth-Science Reviews, 42, 201-229.

Shanmugam, G. (2000) 50 Years of the turbidite paradigm (1950s–1990s): deep-water processes and facies models – a critical perspective. Marine and Petroleum Geology, 17, 285-342

Shanmugam, G. (2002a). Ten turbidite myths. Earth-Science Reviews, 58, 311-341

Shanmugam, G. (2002b). Discussion on Mulder et al. 2001, Geo-Marine Letters, 21, 86–93. Inversely graded turbidite sequences in the deep Mediterranean. A record of deposits from flood-generated turbidity currents? Geo-Marine Letters, 22, 108–111.

Shanmugam, G. (2003). Deep-marine tidal bottom currents and their reworked sands in modern and ancient submarine canyons. Marine and Petroleum Geology, 20, 471-491.

Shanmugam, G. (2006|. Deep-water Processes and Facies Models, Implications for Sandstone Petroleum Reservoirs. Handbook of Petroleum Exploration and Production, vol. 5. Elsevier, Amsterdam, 476

Shanmugam, G., (2012). New Perspectives on Deep-water Sandstones, Origin, Recognition, Initiation, and Reservoir Quality. Handbook of Petroleum Exploration and Production, vol. 9. Elsevier, Amsterdam, 524.

Shanmugam, G. (2013). Modern internal waves and internal tides along oceanic pycnoclines: challenges and implications for ancient deep-marine baroclinic sands. AAPG Bulletin, 97, 767-811

Shanmugam, G. (2016a). The seismite problem. Journal of Palaeogeography, 5(4), 318-362.

Shanmugam, G. (2016b). The Contourite Problem. In: Mazumder, R. (ed.), Sediment Provenance. Elsevier, 183-254. Chapter 9.

Shanmugam, G. (2016c). Submarine fans: A critical retrospective (1950-2015). Journal of Palaeogeography, 5(2), 110-184.

Shanmugam, G. (2017). Contourites: Physical oceanography, process sedimentology, and petroleum geology. Petroleum Exploration and Development, 44(2), 183-216.

Shanmugam, G. (2018a). Comment on "Ichnological analysis of contourites: Past, present and future" by Francisco J. Rodríguez-Tovar and F. Javier Hernandez-Molina [Earth-Science Reviews, 182 (2018), 28–41]. Earth-Science Reviews, 184, 46-49.

Shanmugam, G. (2018b). The hyperpycnite problem. Journal of Palaeogeography, 7 (3), 197-238.

Shanmugam, G.. (2018c). A global satellite survey of density plumes at river mouths and at other environments: Plume configurations, external controls, and implications for deep-water sedimentation. Petroleum Exploration and development, 45 (4), 640-661.

Shanmugam, G., Spalding, T.D., and Rofheart, D.H. (1993). Process sedimentology and reservoir quality of deep-marine bottom-current reworked sands (sandy contourites): an example from the Gulf of Mexico. AAPG Bulletin, 77, 1241-1259

Shanmugam, G., Lehtonen, L.R., Straume, T., Syversten, S.E., Hodgkinson, R.J., and Skibeli, M. (1994). Slump and debris flow dominated upper slope facies in the cretaceous of the Norwegian and northern north Seas (61°–67° N): implications for sand distribution. AAPG Bulletin, 78, 910-937

Steel, E., Simms, A.R., Warrick, J. Yokoyama, Y. (2016). Highstand shelf fans: The role of buoyancy reversal in the deposition of a new type of shelf sand body. GSA Bulletin, 128, 1717–1724.

Stow, D.A.V., and Faugéres, J.-C. (2008). Contourite facies and the facies model. In: M. Rebesco , A. Camerlenghi (eds.). Contourites Developments in sedimentology vol. 60. Elsevier Amsterdam, 223-256, Chapter 13

Talley, L. D. (2013). Closure of the global overturning circulation through the Indian, Pacific, and Southern Oceans: Schematics and transports. Oceanography, 26(1), 80-97.

Varnes, D.J. (1958). Landslide types and processes. In: Eckel, E.B. (ed). Landslide and Engineering Practice. Highway Research Board Special Report, 29, 20-47.

Wang, X.H., and Wang, H.J. (2010). Tidal straining effect on the suspended sediment transport in the Huanghe (Yellow River) Estuary, China. Ocean Dynamics, 60, 1273–1283.

Wetzel, A., Werner, F. and Stow, D.A.V. (2008). Bioturbation and biogenic sedimentary structures in contourites. In: Rebesco, M., Camerlenghi, A. (Eds.), Contourites. Developments in Sedimentology Vol. 60, 183–202.

Wright, L.D., Wiseman, W.J., Bornhold, B.D., Prior, D.B., Suhayda, J.N., Keller, G.H., Yang, Z.S. and Fan, Y.B. (1988). Marine dispersal and deposition of Yellow River silts by gravity-driven under flows. Nature, 332, 629–632.

Yang, R., Jin, Z., van Loon, A.J., Han, Z. and Fan, A. (2017). Climatic and tectonic controls of lacustrine hyperpycnite origination in the Late Triassic Ordos Basin, central China: implications for unconventional petroleum development. AAPG Bulletin, 101 (1), 95–117.

Zavala, C. and Arcuri, M. (2016). Intrabasinal and extrabasinal turbidites: Origin and distinctive characteristics. Sedimentary Geology, 337, 36–54.

Zenk, W., (2008). Abyssal and contour currents. In: Rebesco, M., Camerlenghi, A. (eds.), Contourites. Elsevier, Amsterdam, Developments in Sedimentology 60, 37-57. Chapter 4.

Zhao, J., Jin, Z., Jin, Z., Wen, X., Geng, Y., Yan, C., Nie, H. (2017). Depositional environment of shale in Wufeng and Longmaxi Formations, Sichuan Basin. Petroleum Research, 2, 209-221.